Enhancement of electro-optical response of photonic crystal fibers infiltrated with ferroelectric liquid crystal doped with titanium dioxide nanoparticles

D. Budaszewski, Dharmendra Pratap Singh, T. Woliński

Research Article Vol. 31, No. 18 / 28 Aug 2023 / Optics Express 29942
Optics EXPRESS

Enhancement of electro-optical response of photonic crystal fibers infiltrated with ferroelectric liquid crystal doped with titanium dioxide nanoparticles

D. Budaszewski,[1,*] D. P. Singh,[2] and T. R. Woliński[1]

[1] Faculty of Physics, Warsaw University of Technology, Koszykowa 75, Warszawa, Poland
[2] Unité de Dynamique et Structure des Matériaux Moléculaires (UDSMM), Université du Littoral Côte d'Opale (ULCO), 62228 Calais, France
[*] daniel.budaszewski@pw.edu.pl

Abstract: Light propagation has been studied in photonic crystal fibers (PCFs) doped with W212 ferroelectric liquid crystal (FLC) composites with titanium dioxide nanoparticles (TiO_2 NPs) of low concentrations between 0.2 and 1 wt. % in the FLC matrix. Optical microscopy observations indicated a slight increase of transition temperature to the isotropic phase by ~1–2°C compared to the undoped FLC sample, and the TiO_2 admixture was found to decrease free ionic charge impurities in the FLC, thus improving its electro-optical parameters. The switching time measurements in the PLCFs clearly indicate that TiO_2 NPs reduce switching times for low electric field intensity, even by 32% compared to the undoped PLCF.

1. Introduction

Photonic crystal fibers (PCF) [1] have become essential for modern fiber-optic telecommunication and photonics over the last two decades. Rapid progress in designing and fabricating PCFs resulted in various configurations of fibers exhibiting i.a. high nonlinearity, low attenuation, or a single-mode guiding mechanism. Moreover, PCF-based devices for sensing and tuning applications became especially attractive by infiltrating microholes in the PCF cladding with liquid crystals (LCs) [2–8]. Such optical waveguides that combine properties of both PCFs and LCs are called photonic liquid crystal fibers (PLCFs). The opportunities of LC materials for applications in PCFs have been so far widely investigated for nematic LCs (NLCs) [2–8], their chiral analogs, i.e. cholesteric LCs [9], and blue phase LCs [10–13] that exhibit a local three-dimensional double-twist molecular alignment. Due to high dielectric anisotropy of NLCs, their typical electro-optical response times are in a range of tens to hundreds of milliseconds. Chiral smectic C* LCs, also known as ferroelectric liquid crystals (FLCs) due to their inherent ferroelectricity within the helical structure, exhibit much faster electro-optical response times, even below the microsecond range. The practical applications of FLCs in photonic technology have been recently reviewed elsewhere [14]. Hence, FLCs are promising materials for controlling light guiding in PLCFs. Wong et al. [15] described the sub-millisecond electro-optical switching in a hollow-core PCF infiltrated with an FLC. However, the investigated PLCF system exhibited strong light scattering, making the hollow-core PCF ineffective for developing PLCF-based optical devices. Solid-core PCFs, with FLCs embedded in microholes that form the cladding, are expected to have more considerable potential. Mathews et al. [16] proposed a notch filter based on a PCF infiltrated with an FLC controlled by d.c. electric field. Yu et al. [17] presented a detailed report on the electro-optical characteristics of an FLC embedded in PCFs. It has been seen that the recent studies were focused on the proper alignment of FLC molecules in

#493064 https://doi.org/10.1364/OE.493064
Journal © 2023 Received 24 Apr 2023; revised 19 Jul 2023; accepted 26 Jul 2023; published 25 Aug 2023

Optics EXPRESS

cylindrical structures and the nature of the switching mechanism under the influence of an external electric field [18–20]. Further development of PLCF-based devices requires new LC materials or composites with desired electro-optical parameters. In general, LC materials synthesized in chemical laboratories require extensive studies of their electro-optical behavior, which may be a very complex and time-consuming procedure. Another approach relies on doping existing LC materials with different types of nanoparticles (NP), which seems to be a relatively more straightforward and cost-effective method. The admixture of NPs in the LCs can largely modify their parameters, as phase transition temperatures, optical and dielectric anisotropies, as well elastic constants. The presence of NPs in FLCs can also have a significant impact on their tilt angle, spontaneous polarization, helix pitch and rotational viscosity. However, it should be noted that NPs can also affect stability of the FLC phase. It was reported [21] that admixture of the Fe_2O_3 NPs in a EHPBD FLC material caused an electrohydrodynamic instability in the FLC-NP nanocomposite in the form of elongated domains observed in the glass cell. This effect has been descried in details in [22]. Moreover, the size of the NPs in an FLC volume can also impact the orientation stability of the FLC-NP nanocomposite [23]. Nevertheless, over the last few years, much research has proven great potential of LC-NP nanocomposites in glass cells, micro capillaries, and PCFs. It was found that gold and silver NPs dispersed in NLCs have a positive impact on PLCF properties by reducing their switching times and threshold voltages [24–26]. However, the specific type of NPs, i.e., metallic, dielectric, and ferroelectric, as well as their shape and surface coating, may also worsen LC-NP electro-optical parameters [27–30]. Consequently, the impact of NPs dispersed in FLCs has also been widely studied. It was reported that silica NPs dispersed in FLCs may improve the electro-optical switching times [31]. Kumar et al. have observed that palladium NPs positively impacted the FLC-NP nanocomposite's electro-optical and dielectric characteristics [32,33]. Experiments on the influence of gold NPs embedded in FLC showed a significant increase in the optical tilt [34] and enhancement of photoluminescent properties [35]. A detailed review of the interaction of gold NPs on FLC was presented by Choudhary [36]. The preparation, stability and long-term durability of Au and Ag types of NPs are not so facile to use in devices due to their oxidizing nature; therefore, other alternative NPs must be developed. Lalik et al. doped FLC with Fe_2O_3 NPs and showed that even small concentration of the NPs leads to a significant decrease of the spontaneous polarization, tilt angle, rotational viscosity, and switching times [21].

In recent years titanium dioxide (TiO_2) NPs have also exhibited significant potential in doping FLCs. The main advantage of TiO_2 NPs is their ability to suppress free ionic charges generally present in LCs. The presence of these impurities negatively influences the performance of LC-based optical devices. Gupta et al. reported [37] that TiO_2 NPs when dispersed in FLCs lead to reduced d.c. conductivity, increased spontaneous polarization, and cause switching times enhancement of FLC-NP nanocomposites. Usually, TiO_2 NPs have been utilized in LCs to filter ionic impurities [38], changing luminescence [39] and improving the response time of nematics [40]; however, their use in PLCFs could result in some important characteristics.

The present work describes further research efforts toward applying TiO_2 NPs as dopants in FLCs and subsequent impact on PLCFs' electro-optical properties.

2. Experimental

As a geometrically confining medium for current studies, we used an LMA-10 PCF manufactured by NKT Photonics. The LMA-10 photonic lattice consists of six rings of hollow microcappilaries (MCs) with an internal diameter $d = 2.84$ μm surrounding a solid core. The distance between MCs, referred as pitch, is equal to $\Lambda = 6.48$ μm. Both values were measured under an SEM microscope (Hitachi TM4000) and presented in Fig. 1.

The FLC selected for the present studies was W212 FLC (synthesized at the Military University of Technology) characterized by its helical pitch $p = 7$ μm, spontaneous polarization $P_s = 100$

Optics EXPRESS

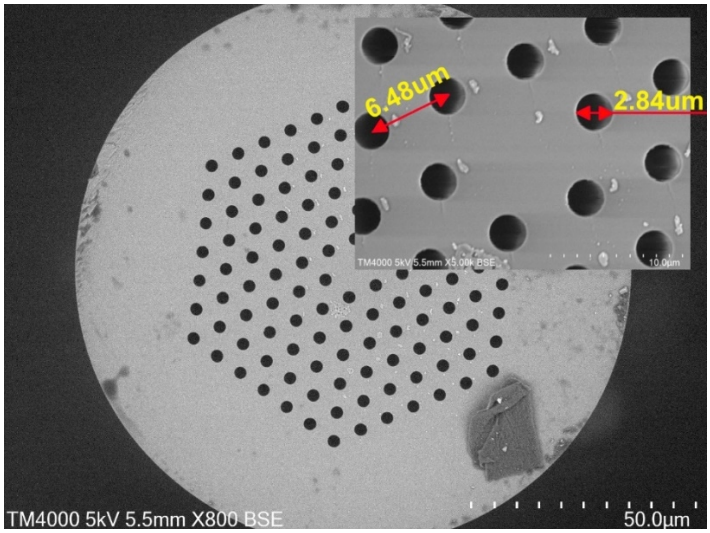

Fig. 1. Cross-section of the LMA10 PCF. The inset represents the dimensions of the microholes, d and the pitch, Λ.

nC/cm^2, and a tilt angle $\theta = 40°$ (as measured at room temperature). The phase transition scheme for W212 FLC is as follows: Cr 10°C SmC* 99.8°C SmA* 126.6°C Iso [41–43]. The titanium dioxide nanoparticles (TiO_2 NPs) existed in an anatase form and were prepared according to the method described in [39,44]. The size of the NPs was in a range of 25-35 nm. Hereafter, we present the details of preparing the samples and methods used in our studies.

2.1. Preparation of the W212 doped with titanium dioxide NPs

To prepare each nanocomposite sample, first TiO_2 NPs were mixed with toluene and left for ultrasonication for 2 hours to ensure a uniform distribution of the TiO_2 NPs in the mixture. Colloid homogeneity was examined by leaving the sample for 24 hours. Next, the TiO_2 solution was added to the W212 FLC in three different amounts to maintain 0.2, 0.5, and 1.0% wt./wt. concentrations. Low NPs concentrations provided an undistorted FLCs molecular order and the director's direction in each smectic layer. Moreover, the NPs can have non-zero dipole moments, and their interactions may result in uncontrolled aggregation for higher concentrations [45]. It should be emphasized that the proper stirring procedure of the FLC-NP mixture may provide an average distance between the NPs, large enough to avoid any aggregations of the dopant particles [46].

After that, the sample was again left for ultrasonication for additional 2 hours and then placed in an oven at a temperature of 70°C to evaporate toluene completely from the samples.

2.2. Preparation of the MC and PCF doped with W212 - TiO_2 admixture

In the preparatory stage, the inner walls of the 12-µm in diameter MC and the LMA10 PCF were covered with photosensitive sulfonic azo-dye SD1 [47–49] as a photo-aligned layer, necessary for the proper alignment of the FLC-NPs nanocomposites. The detailed procedure of generating the photo-aligned layer and infiltration with the FLC mixture has been previously reported elsewhere [18]. It should be emphasized that application of SD1 layers in both cylindrical and planar structures can provide an excellent alignment for different LCs, under the condition that the photo-aligning layer has a proper thickness. As reported by Pozhidaev et al. [50], the thickness of the SD1 layer strongly depends on the concentration of the SD1 azo-dye in the solvent. The

Optics EXPRESS

thickness of the SD1 layer could be performed by the atomic force method. This method can give precise results on glass substrates, but in case of media with cylindrical geometry, the measurements may be incorrect. In our research, we used a 5% solution of SD1 in DMF solvent, and based on calculations given in [50] we estimated that the SD1 layer thickness in MC and PCF should be approx. 50 nm.

Before MC and PCF infiltration, the FLC-NP nanocomposite was stirred by using a sonification process in order to avoid possible aggregations.

Afterwards, the MC and LMA10 PCFs were dipped in the containers with W212-TiO_2 nanocomposites with different concentrations and left for approximately 40 minutes in the oven at a temperature of 140°C, at which W212 remains in the isotropic phase.

After that, the quality of infiltrations and nanocomposite alignment was observed under a polarizing microscope. Next, 5-mm long infiltrated PCF samples were placed in the capillary with an inner diameter of 126 µm using a micromechanical setup and two SM fibers were introduced as input and output on both sides of the microcapillary. Both SM fibers were joined to the microcapillary by using a UV-curable glue. We believe this method is better than that of fusion-splicing so as to avoid the destruction of the FLC-NP nanocomposite by high temperature.

2.3. Characterization of the spontaneous polarization

One of the FLCs' crucial parameters is their spontaneous polarization. Usually, this parameter decreases with increasing temperature and disappears at the SmC*-SmA phase transition. The spontaneous polarization measurements were performed in 3 µm-thick ITO coated glass cells infiltrated with NP-FLC nanocomposites using the setup presented in Fig. 2 [51].

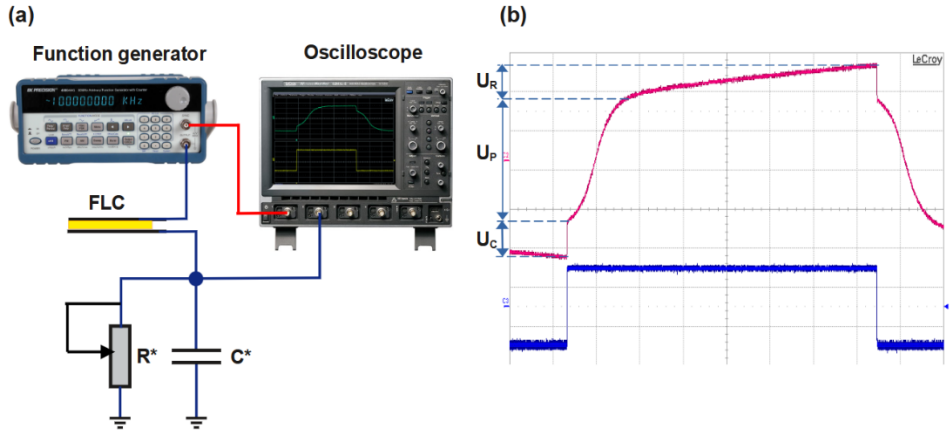

Fig. 2. Schematic diagram of the setup for measuring electro-optical parameters of FLC samples (a) and an exemplary oscillogram representing the response signal across the capacitance C* and driving signal from a function generator. The resistance R* was adjusted by 10 kΩ potentiometer and the capacitance C* was 2.2 µF.

The response signal U_{OUT} consists of three voltage components and is defined according to the formula 1 [52]

$$U_{OUT} = U_R + U_C + U_P = \frac{1}{C^*}\int_0^t I\,dt = \frac{Ut}{RC^*} + \frac{2UC_{FLC}}{C^*} + \frac{P_S S}{C^*}[\cos(\varphi(t)) - \cos(\varphi_0)] \quad (1)$$

where: U_R is related to the resistivity of the cell, U_C corresponds to the capacitance of the cell, U_P is the repolarization voltage caused by polarization reversal, R* is the ohmic resistance of the cell, S is the area of the FLC layer in the cell, C* is the reference capacitance connected in series

Optics EXPRESS

with the cell, $\varphi_0 = \varphi(t = 0)$ is the initial azimuthal angle of the FLC molecules in the cell. The oscillogram showing the driving signal and the response signal U_{OUT} in this method is presented in Fig. 2.

According to the Eq. (1), spontaneous polarization can be calculated by measuring voltage U_P:

$$P_S = \frac{U_P C^*}{S[\cos(\varphi(t)) - \cos(\varphi_0)]} \tag{2}$$

In our setup, a 2.2 µF reference capacitor was used, and the voltage U_R was continuously compensated by the 10 kΩ potentiometer.

2.4. Characterization of phase changes in the temperature regime

Phase transition temperatures were measured under a polarizing microscope (Nikon T2sAr) with crossed polarizers. The 12-µm silica-glass MCs were treated with an SD1 photo-aligning material, according to the description from [18], and infiltrated with the investigated FLC-NP nanocomposites. We estimated the beginning and end of the phase transition temperatures through optical observations. A computer-controlled hot stage (Linkam TM6000) was utilized to precisely control the temperature of the samples over the range from 50°C to 130°C with a resolution of 1°C/min.

2.5. Characterization of guiding properties

Light propagation in PCFs infiltrated with LCs is governed by a photonic bandgap guiding mechanism that results from generally higher refractive indices of the LC material in comparison to the refractive index of the PCF (silica glass). Light guiding studies were performed by using a broadband halogen lamp (Mikropak, HL-2000) and an optical spectrum analyzer (Ocean Optics, USB2000). Moreover, the infiltrated part of the samples was placed on the Peltier module to investigate spectral changes under the influence of temperature in the range from 20°C to

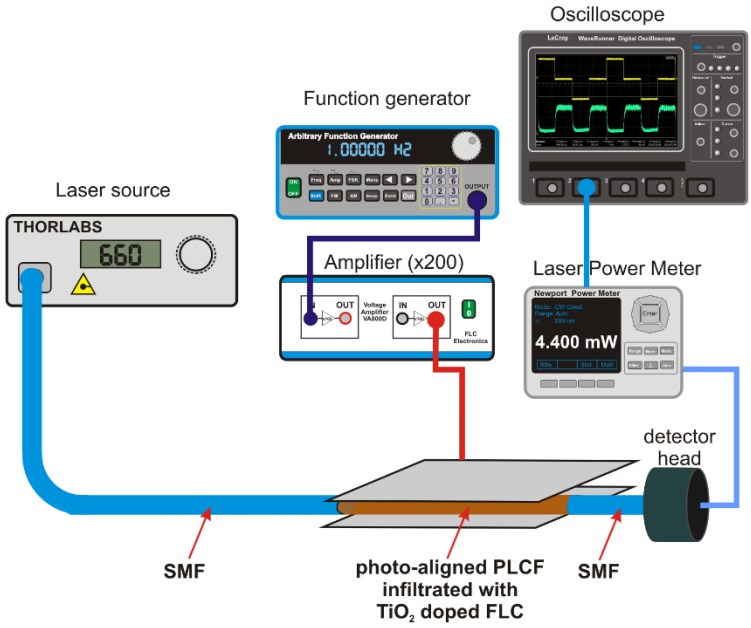

Fig. 3. Experimental setup for measuring electro-optical response under the influence of the external electric field.

Optics EXPRESS

80°C. The temperature of the sample was measured by a digital thermometer (Testo 735) with a resolution of 0.1°C.

2.6. Characterization of the response times

The crucial point of interest was to investigate whether the presence of TiO_2 NPs can influence electro-optical response times in the PLCF samples. The experimental setup used in this part is presented in Fig. 3.

A monochromatic laser beam operating at 660 nm was selected for this study since all investigated PLCF samples had relatively good propagation properties at this wavelength. The infiltrated part was placed between two metal electrodes connected to a function generator supplying a square-shaped signal at 10 Hz (Rigol DG1022A) through a voltage amplifier (FLC A800DI). The distance between electrodes was estimated to be 130 µm, which corresponds to a maximum electric field intensity up to 5.5 V/µm. The response signal was collected by an optical power meter (Newport 2936-R) and visualized on a digital oscilloscope (LeCroy 104MXi).

3. Results and discussion

Electro-optic response of photoaligned FLCs can be significantly improved by proper selection of the FLC's physical parameters. Switching times in FLCs can be defined by the rotational viscosity that corresponds to the energy dissipation in the director reorientation process under the influence of driving electric field. One of the possible ways to increase switching times in FLCs includes minimizing of the viscosity with a simultaneous rise in spontaneous polarization. However, an increase in spontaneous polarization may not be compatible with the lower values of rotational viscosity. Moreover, the FLCs' helix pitch is another important parameter responsible for the electro-optical optimization. This parameter can be easily modified by dispersing chiral dopants in the FLC matrix [53]. As reported in [50], for photo-aligning purposes, the most preferable are helix-free FLC materials. This condition can be true not only for plain glass cells, but also for host materials with cylindrical geometry as PCFs.

However, as mentioned in the introduction, selection of the optimal FLC physical parameters requires extensive studies and may be time-consuming. Hence, our approach was to investigate the influence of TiO_2 NPs on FLC electro-optical parameters. In the following section, the results of our research are provided and discussed.

3.1. Spontaneous polarization

As reported in section 2.3, the setup described in [51] was used to calculate the spontaneous polarization as a function of an externally applied electric field, at a frequency of 20 Hz and temperature of 20°C. The variation of spontaneous polarization for electric field intensities ranging from 1 V/µm to 4 V/µm is presented in Fig. 4.

As shown in Fig. 4, the presence of TiO_2 NPs significantly increased the W212 spontaneous polarization for low intensities of the electric field. This phenomenon can be attributed to the trapping of free ionic charges present in FLC by TiO_2 NPs [37]. As a result, the polarization component of FLC molecules can be aligned easier along the electric field lines leading to higher values of spontaneous polarization.

For higher electric field intensities, the value of spontaneous polarization reaches a similar value for the all investigated W212-TiO_2 nanocomposites. This effect suggests that the presence of free ionic charges has been reduced to minimum and any other improvement of spontaneous polarization is no longer possible. It also indicates weak interactions between W212 molecules and TiO_2 NPs in the nanocomposite. It should be noted that the opposite effect has been reported by Kumar et al. [54], where doping TiO_2 NP to the W206 FLC resulted in a decrease in spontaneous polarization. A possible explanation for this result can be attributed to a different molecular structure of the FLC material.

Optics EXPRESS

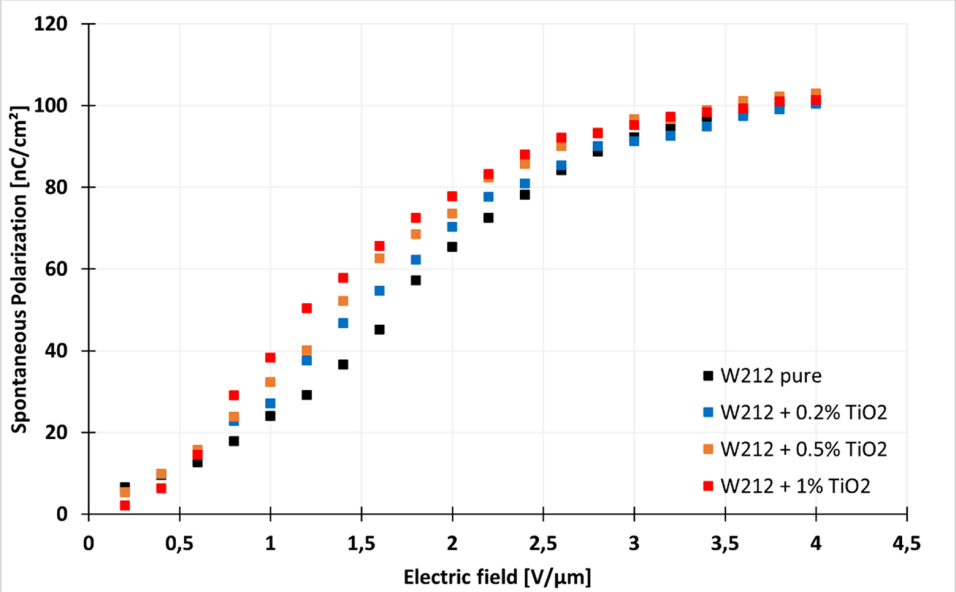

Fig. 4. Temperature dependence of spontaneous polarization for the W212 FLC: undoped and doped with a TiO_2 admixture.

3.2. *Phase changes under the thermal regime*

Thermal observations were performed to investigate the phase transition between liquid crystal state and isotropic state for undoped and TiO_2-doped W212 FLC in 12-µm MCs. Since the phase transition takes more time in cylindrical structures than in planar structures, we reported two temperatures corresponding to the beginning and end of the phase transition process (Fig. 5).

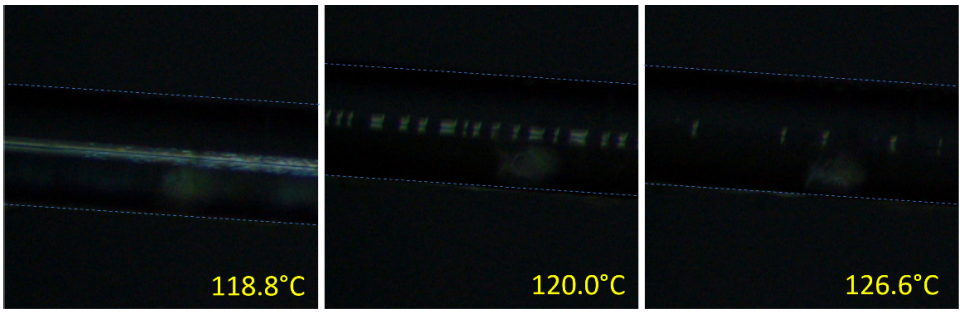

Fig. 5. The beginning and end of liquid crystal - isotropic phase transition for nanocomposite W212 with 0.5% wt. TiO_2 admixture observed in the 12-µm microcapillary.

As shown in Table 1, a slight increase in a phase transition temperature of ~1 - 2 °C has been observed for W212 doped with TiO_2 NPs. A similar effect of increasing the phase transition temperature for higher concentrations of the NPs in various LC materials was reported by other research groups. As it was presented elsewhere [55], the doping of the BL011nematic LC (NLC) with a silica NP slightly increased phase transition temperature. According to the authors of [55], it was caused by a non-uniform distribution of silica NPs in the nematic material, which enhanced the local orientational order of NLC. Similarly, incorporating carbon nanotubes into E7 NLC [56] increased the phase temperature, which was attributed to the anisotropic alignment

Optics EXPRESS

of LC along the carbon nanotubes bundles. Li *et al.* [57] studied the influence of ferroelectric $BaTiO_3$ NPs in NLC that resulted in a noticeable increase in the phase transition temperature. The observed effect has been attributed to the presence of $BaTiO_3$ NPs that amplified LC orientational coupling. However, doping NLCs and FLCs with metallic NPs can have an opposite effect leading to lowering the phase transition temperature for higher concentrations of the NP dopant. As reported in the previous studies [26,58], doping a 6CHBT NLC with gold NPs caused the lowering of nematic-isotropic phase transition. The same effect was observed for 6CHBT NLC doped with silver NPs, where the phase transition temperature decreased even by 3°C for higher concentrations of silver NPs. Further studies [59] reported a decrease in phase transition temperature for the W212 FLC doped with gold NPs.

Table 1. Mesophase-isotropic phase transition for a 12-µm MC infiltrated with a W212-TiO_2 nanocomposite

Material	Beginning of the phase transition [°C]	End of the phase transition [°C]
W212	117.6	125.1
W212 + 0.2% TiO_2	118.5	125.8
W212 + 0.5% TiO_2	118.8	126.6
W212 + 1% TiO_2	119.5	126.9

3.3. Light guiding in the PLCF samples

Light-guiding properties were examined by using the setup described in section 2.5 to select the best wavelength for further electro-optical measurements. Moreover, we have analyzed the thermal influence on resulting light spectrum guided through our samples.

As shown in Fig. 6, a shift towards shorter wavelengths can be observed by increasing the temperature of the PLCF samples. For undoped PLCF, the shift of the dominant maximum, as a function of temperature, is equal to 38 nm, while for 1% wt. concentration in PLCF, the shift value was even 54 nm. It can be concluded that the light spectrum guided inside the PLCF can be influenced by the presence of TiO_2 NPs dispersed in FLC. For all investigated PLCFs, the maximum of light propagation can be registered for wavelengths within a range of 600-700 nm for all temperatures. As our studies were performed in a temperature of 20°C, we chose a laser diode (LD) operating at a wavelength of 660 nm for further electro-optical measurements, since for this wavelength we observe relatively good propagation.

3.4. Switching times

The switching time is assumed as the time required to change the value of the signal from 10% to 90% (or vice versa) of its maximum value. We have performed the measurements for all investigated PLCF samples using the setup shown in Fig. 3. The obtained results are presented in Fig. 7.

Shown in Fig. 7, the significant improvement in switching times is observed for low electric field intensities. For 0.2% wt. concentration of TiO_2 NPs in PLCF, the switching times in the range of low electric field values are approximately 8-11% faster compared to the undoped PLCF sample. By increasing the intensity of external electric field over 3.5 V/µm, the percentage change of time value drops to 5-7%. A similar effect is registered for higher concentrations of TiO_2 NPs. For 0.5% wt. concentration of TiO_2 NPs, the switching time for lower field values is 15-19% faster than for undoped PLCF, and for higher electric field values, one can achieve 8-11% improvement in the switching times. The best results of switching times improvement are observed for the 1% wt. concentration of the TiO_2 NPs in the PLCF. For lower electric fields, the switching times drop even to 25-32% compared to undoped PLCF, and for the electric

Optics EXPRESS

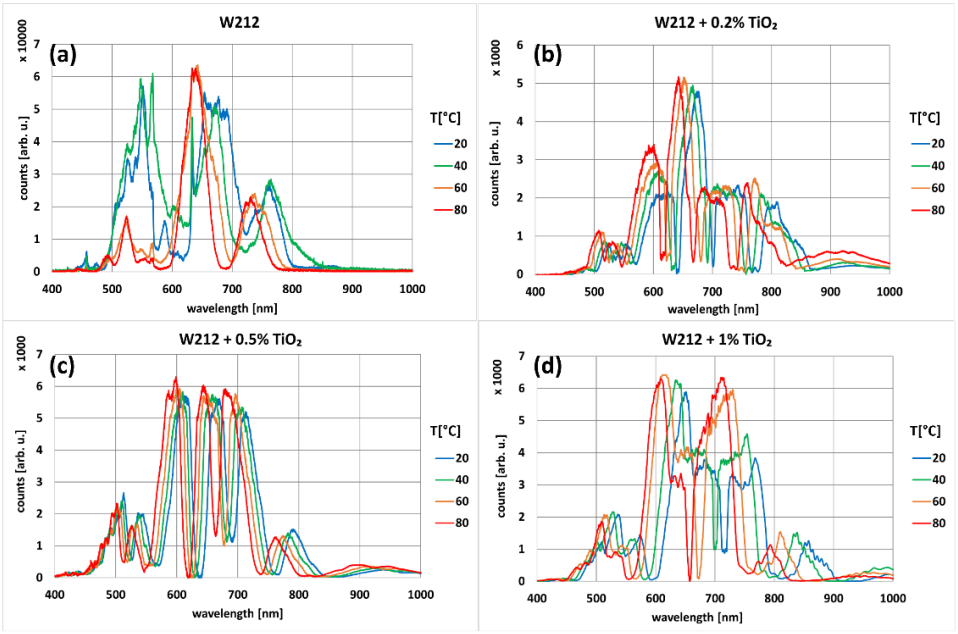

Fig. 6. Light spectra of the PLCFs infiltrated with (a) undoped W212 FLC and with TiO_2 dopant at concentrations of (b) 0.2% wt., (c) 0.5% wt. and (d) 1% wt. measured in the thermal range: 20°C -80°C.

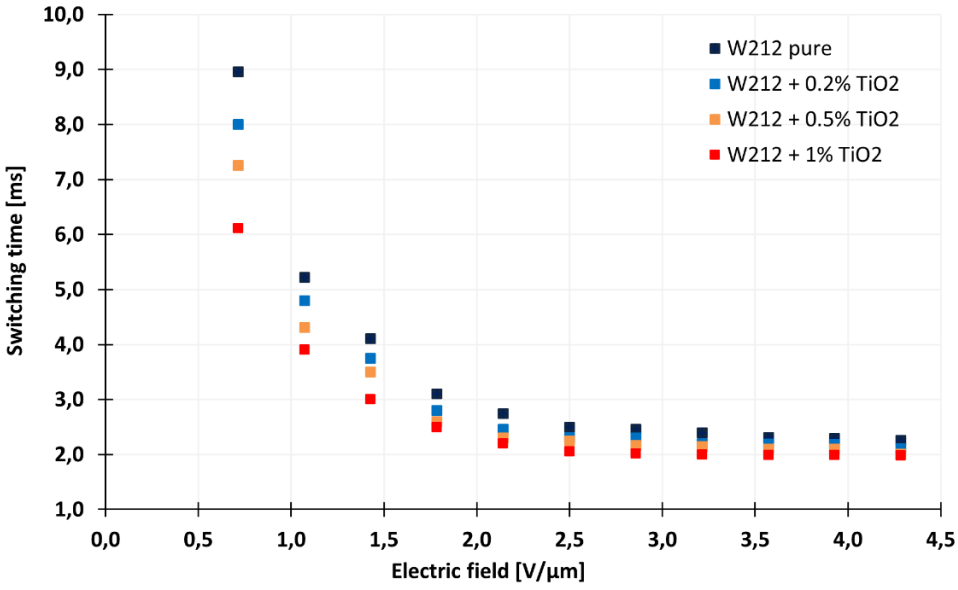

Fig. 7. Switching times registered for undoped W212 FLC and with three concentrations of TiO_2 NP.

Optics EXPRESS

field over 3 V/μm, the drop is 12-14% faster than in undoped PLCF. However, for higher values of electric field intensity, only a small improvement in switching time can be noticed. This behavior is directly related to the characteristic of the spontaneous polarization presented in Fig. 4. The significant differences in spontaneous polarization for low-electric fields result in significant variations of the switching time. Hence, that indicates that PLCF infiltrated with W212 doped with a high concentration of TiO_2 NPs is faster in comparison to PLCF infiltrated with pure W212 FLC. In the case of higher electric field intensities, the variation of spontaneous polarization for all PLCF samples was minimal suggesting that the registered switching times would not differ significantly. It can be concluded that TiO_2 NPs can be considered as a suitable dopant for FLC-based in-fiber devices for prospective photonic applications.

4. Conclusions

We have investigated the influence of TiO_2 NPs on the electro-optical parameters of the W212 FLC infiltrating the LMA-10 PCF. The obtained results indicate that spontaneous polarization of the W212 FLC can be increased by the presence of the TiO_2 NPs, but only for low electric field intensities. This can be attributed to the trapping of free ionic charges by TiO_2 NPs in the FLC-NP nanocomposites. which leads to an improvement in spontaneous polarization values. The switching time measurements in the PLCFs clearly reveal that TiO_2 NPs exhibit a positive impact on the reduction of switching times for low intensities of electric field, even up to 32%, in comparison to undoped PLCF. It can be concluded that TiO_2 NPs can be considered as a suitable material for modification of the electro-optical properties of the FLC-based in-fiber devices for modern photonics systems.

Funding. Politechnika Warszawska (CB POB FOTECH 2); Narodowe Centrum Nauki (NCN 2011/03/B/ST7/02547).

Acknowledgment. DB would like to thank Prof. Vladimir Chigrinov (HKUST, Hong Kong, SAR China) for supplying SD1 material. DPS is thankful to POLE MTE of the ULCO for the financial support. Research was funded by CB POB FOTECH of Warsaw University of Technology within the Excellence Initiative: Research University (IDUB) programme.

Disclosures. The authors declare that there are no conflicts of interest related to this article.

Data availability. Data underlying the results presented in this paper are not publicly available at this time but may be obtained from the authors upon reasonable request.

References

1. P. S. J. Russell, "Photonic-Crystal Fibers," J. Lightwave Technol. **24**(12), 4729–4749 (2006).
2. T. T. Alkeskjold, J. Laegsgaard, A. Bjarklev, D. S. Hermann, A. Anawati, J. Broeng, J. Li, and S.-T. Wu, "All-optical modulation in dye-doped nematic liquid crystal photonic bandgap fibers," Opt. Express **12**(24), 5857–5871 (2004).
3. M. W. Haakestad, T. T. Alkeskjold, M. D. Nielsen, L. Scolari, J. Riishede, H. E. Engan, and A. Bjarklev, "Electrically tunable photonic bandgap guidance in a liquid-crystal-filled photonic crystal fiber," IEEE Photon. Technol. Lett. **17**(4), 819–821 (2005).
4. T. R. Wolinski, A. Czapla, S. Ertman, M. Tefelska, A. W. Domanski, J. Wojcik, E. Nowinowski-Kruszelnicki, and R. Dabrowski, "Photonic Liquid Crystal Fibers for Sensing Applications," IEEE Trans. Instrum. Meas. **57**(8), 1796–1802 (2008).
5. T. R. Woliński, D. Budaszewski, M. Chychłowski, A. Czapla, S. Ertman, P. Lesiak, K. Rutkowska, M. Sierakowski, M. Tefelska, and A. W. Domański, "Photonic liquid crystal fibers: Towards highly tunable photonic devices," in *International Conference on Photonics* (IEEE, 2010), pp. 1–5.
6. A. Lorenz, R. Schuhmann, and H.-S. Kitzerow, "Infiltrated photonic crystal fiber: experiments and liquid crystal scattering model," Opt. Express **18**(4), 3519–3530 (2010).
7. L. Scolari, L. Wei, S. Gauza, S.-T. Wu, and A. Bjarklev, "Low loss liquid crystal photonic bandgap fiber in the near-infrared region," Opt. Rev. **18**(1), 114–116 (2011).
8. A. Lorenz and H.-S. Kitzerow, "Efficient electro-optic switching in a photonic liquid crystal fiber," Appl. Phys. Lett. **98**(24), 241106 (2011).
9. R. Ozaki, N. Uno, and H. Moritake, "Quasi-Two-Dimensional Optical Confinement in a Cholesteric Liquid Crystal Infiltrated Optical Fiber," Jpn. J. Appl. Phys. **50**(11R), 111601 (2011).
10. D. Poudereux, K. Orzechowski, O. Chojnowska, M. Tefelska, T. R. Woliński, and J. M. Otón, "Infiltration of a photonic crystal fiber with cholesteric liquid crystal and blue phase," Proc. SPIE **9290**, 92900A (2014).

Optics EXPRESS

11. R. Dąbrowski, "From the discovery of the partially bilayer smectic A phase to blue phases in polar liquid crystals," Liq. Cryst. **42**(5-6), 1–36 (2015).
12. M. M. Sala-Tefelska, K. Orzechowski, M. Sierakowski, A. Siarkowska, T. R. Woliński, O. Strzeżysz, and P. Kula, "Influence of cylindrical geometry and alignment layers on the growth process and selective reflection of blue phase domains," Opt. Mater. **75**, 211–215 (2018).
13. M. Wahle, J. Ebel, D. Wilkes, and H.-S. Kitzerow, "Asymmetric band gap shift in electrically addressed blue phase photonic crystal fibers," Opt. Express **24**(20), 22718–22729 (2016).
14. S. K. Gupta, D. Budaszewski, and D. P. Singh, "Ferroelectric liquid crystals: futuristic mesogens for photonic applications," Eur. Phys. J. Spec. Top. **231**(4), 673–694 (2022).
15. C. S. I. Wong, J.-Y. Liu, and K. M. Johnson, "Ferroelectric Liquid Crystal Fiber Waveguide," Ferroelectrics **181**(1-4), 61–67 (1996).
16. S. Mathews, Y. Semenova, and G. Farrell, "Electronic tunability of ferroelectric liquid crystal infiltrated photonic crystal fibre," Electron. Lett. **45**(12), 617–618 (2009).
17. J.-S. Yu, J. S. Yu, and J.-H. Kim, "Electro-optical Characteristics of Ferroelectric Liquid Crystal Embedded in Photonic Crystal Fiber," Jpn. J. Appl. Phys. **52**(5R), 051701 (2013).
18. D. Budaszewski, A. K. Srivastava, A. M. W. Tam, T. R. Wolinski, V. G. Chigrinov, and H.-S. Kwok, "Photo-aligned ferroelectric liquid crystals in microchannels," Opt. Lett. **39**(16), 4679–4682 (2014).
19. S. Knust, M. Wahle, and H. S. Kitzerow, "Ferroelectric Liquid Crystals in Microcapillaries: Observation of Different Electro-optic Switching Mechanisms," J. Phys. Chem. B **121**(19), 5110–5115 (2017).
20. D. Budaszewski, A. K. Srivastava, V. G. Chigrinov, and T. R. Woliński, "Electro-optical properties of photo-aligned photonic ferroelectric liquid crystal fibres," Liq. Cryst. **46**(2), 272–280 (2019).
21. S. Lalik, O. Stefańczyk, D. Dardas, N. Górska, S. Ohkoshi, and M. Marzec, "Modifications of FLC Physical Properties through Doping with Fe2O3 Nanoparticles (Part I)," Materials **14**(16), 4722 (2021).
22. L. M. Blinov, M. I. Barnik, V. T. Lazareva, and A. N. Trufanov, "Electrohydrodynamic instabilities in the liquid crystalline phases with smectic ordering," J. Phys. Colloques **40**(C3), C3-263 (1979).
23. A. K. Misra, P. K. Tripathi, K. K. Pandey, F. P. Pandey, S. Singh, and A. Singh, "Electro-optic switching and memory effect in suspension of ferroelectric liquid crystal and iron oxide nanoparticles," Mater. Res. Express **6**(10), 1050d2 (2019).
24. R. Dąbrowski, K. Garbat, S. Urban, T. R. Woliński, J. Dziaduszek, T. Ogrodnik, and A. Siarkowska, "Low-birefringence liquid crystal mixtures for photonic liquid crystal fibres application," Liq. Cryst. **44**(12-13), 1–18 (2017).
25. D. Budaszewski, A. Siarkowska, M. Chychłowski, B. Jankiewicz, B. Bartosewicz, R. Dąbrowski, and T. R. Woliński, "Nanoparticles-enhanced photonic liquid crystal fibers," J. Mol. Liq. **267**, 271–278 (2018).
26. D. Budaszewski, M. Chychłowski, A. Budaszewska, B. Bartosewicz, B. Jankiewicz, and T. R. Woliński, "Enhanced efficiency of electric field tunability in photonic liquid crystal fibers doped with gold nanoparticles," Opt. Express **27**(10), 14260–14269 (2019).
27. F. Li, J. West, A. Glushchenko, C. I. Cheon, and Y. Reznikov, "Ferroelectric nanoparticle/liquid-crystal colloids for display applications," J. Soc. Inf. Disp. **14**(6), 523–527 (2006).
28. A. Glushchenko, C. I. Cheon, J. West, F. Li, E. Büyüktanir, Y. Reznikov, and A. Buchnev, "Ferroelectric Particles in Liquid Crystals: Recent Frontiers," Mol. Cryst. Liq. Cryst. **453**(1), 227–237 (2006).
29. J.-F. Blach, S. Saitzek, C. Legrand, L. Dupont, J.-F. Henninot, and M. Warenghem, "BaTiO3 ferroelectric nanoparticles dispersed in 5CB nematic liquid crystal: Synthesis and electro-optical characterization," J. Appl. Phys. **107**(7), 074102 (2010).
30. S. Klein, R. M. Richardson, R. Greasty, R. Jenkins, J. Stone, M. R. Thomas, and A. Sarua, "The influence of suspended nanoparticles on the Frederiks threshold of the nematic host," Phil. Trans. R. Soc. A. **371**(1988), 20120253 (2013).
31. A. Chaudhary, P. Malik, R. Mehra, and K. K. Raina, "Electro-optic and dielectric studies of silica nanoparticle doped ferroelectric liquid crystal in SmC* phase," Phase Transit. **85**(3), 244–254 (2012).
32. A. Kumar, G. Singh, T. Joshi, G. K. Rao, A. K. Singh, and A. M. Biradar, "Tailoring of electro-optical properties of ferroelectric liquid crystals by doping Pd nanoparticles," Appl. Phys. Lett. **100**(5), 054102 (2012).
33. A. Kumar, G. Singh, T. Joshi, and A. M. Biradar, "Electro-optical and dielectric characteristics of ferroelectric liquid crystal dispersed with palladium nanoparticles," J. Mol. Liq. **315**, 113776 (2020).
34. S. Kaur, S. P. Singh, A. M. Biradar, A. Choudhary, and K. Sreenivas, "Enhanced electro-optical properties in gold nanoparticles doped ferroelectric liquid crystals," Appl. Phys. Lett. **91**(2), 023120 (2007).
35. A. Kumar, J. Prakash, D. S. Mehta, A. M. Biradar, and W. Haase, "Enhanced photoluminescence in gold nanoparticles doped ferroelectric liquid crystals," Appl. Phys. Lett. **95**(2), 023117 (2009).
36. A. Choudhary, G. Singh, and A. M. Biradar, "Advances in gold nanoparticle–liquid crystal composites," Nanoscale **6**(14), 7743–7756 (2014).
37. S. Kumar Gupta, D. P. Singh, and R. Manohar, "Electrical And Polarization Behaviour Of Titania Nanoparticles Doped Ferroelectric Liquid Crystal," Adv. Mater. Lett. **6**(1), 68–72 (2015).
38. S. P. Yadav, M. Pande, R. Manohar, and S. Singh, "Applicability of TiO2 nanoparticle towards suppression of screening effect in nematic liquid crystal," J. Mol. Liq. **208**, 34–37 (2015).

Optics EXPRESS

39. D. P. Singh, K. Agrahari, A. S. Achalkumar, C. V. Yelamaggad, R. Manohar, and M. Depriester, "Preparation and photophysical properties of soft-nano composites comprising guest anatase TiO 2 nanoparticle and host hekates mesogens," J. Lumin. **205**, 304–309 (2019).
40. B. P. Singh, C.-Y. Huang, D. P. Singh, P. Palani, B. Duponchel, M. Sah, R. Manohar, and K. K. Pandey, "The scientific duo of TiO2 nanoparticles and nematic liquid crystal E204: Increased absorbance, photoluminescence quenching and improving response time for electro-optical devices," J. Mol. Liq. **325**, 115130 (2021).
41. K. Kurp, M. Czerwiński, and M. Tykarska, "Ferroelectric compounds with chiral (S)-1-methylheptyloxycarbonyl terminal chain – their miscibility and a helical pitch," Liq. Cryst. **42**(2), 248–254 (2015).
42. K. Kurp, M. Czerwiński, M. Tykarska, and A. Bubnov, "Design of advanced multicomponent ferroelectric liquid crystalline mixtures with submicrometre helical pitch," Liq. Cryst. **44**(4), 748–756 (2017).
43. K. Kurp, M. Czerwiński, M. Tykarska, P. Salamon, and A. Bubnov, "Design of functional multicomponent liquid crystalline mixtures with nano-scale pitch fulfilling deformed helix ferroelectric mode demands," J. Mol. Liq. **290**, 111329 (2019).
44. B.-X. Lei, Q.-P. Luo, X.-Y. Yu, W.-Q. Wu, C.-Y. Su, and D.-B. Kuang, "Hierarchical TiO2 flowers built from TiO2 nanotubes for efficient Pt-free based flexible dye-sensitized solar cells," Phys. Chem. Chem. Phys. **14**(38), 13175–13179 (2012).
45. R. Basu and A. Garvey, "Effects of ferroelectric nanoparticles on ion transport in a liquid crystal," Appl. Phys. Lett. **105**(15), 151905 (2014).
46. O. P. Pishnyak, S. V. Shiyanovskii, and O. D. Lavrentovich, "Inelastic Collisions and Anisotropic Aggregation of Particles in a Nematic Collider Driven by Backflow," Phys. Rev. Lett. **106**(4), 047801 (2011).
47. M. Schadt, K. Schmitt, V. Kozinkov, and V. Chigrinov, "Surface-Induced Parallel Alignment of Liquid Crystals by Linearly Polymerized Photopolymers," Jpn. J. Appl. Phys. **31**(7R), 2155–2164 (1992).
48. V. Chigrinov, S. Pikin, A. Verevochnikov, V. Kozenkov, M. Khazimullin, J. Ho, D. D. Huang, and H.-S. Kwok, "Diffusion model of photoaligning in azo-dye layers," Phys. Rev. E **69**(6), 061713 (2004).
49. V. G. Chigrinov, V. M. Kozenkov, and H.-S. Kwok, *Photoalignment of Liquid Crystalline Materials* (John Wiley & Sons, Ltd., 2008).
50. E. Pozhidaev, V. Chigrinov, D. Huang, A. Z. Ho, and H. S. Kwok, "Photoalignment of Ferroelectric Liquid Crystals by Azodye Layers," Jpn. J. Appl. Phys. **43**(8R), 5440 (2004).
51. V. Vaksman and Y. Panarin, "Measurement of Ferroelectric Liquid Crystal Parameters," 1, 147–154 (1992).
52. V. Panov, J. K. Vij, and N. M. Shtykov, "A field-reversal method for measuring the parameters of a ferroelectric liquid crystal," Liq. Cryst. **28**(4), 615–620 (2001).
53. L. M. Blinov and V. G. Chigrinov, *Electrooptic Effects in Liquid Crystal Materials* (Springer, 1994).
54. P. Kumar, A. Kishore, and A. Sinha, "Effect Of Different Concentrations Of Dopant Titanium Dioxide Nanoparticles On Electro-optic And dielectric Properties Of Ferroelectric Liquid Crystal Mixture," Adv. Mater. Lett. **7**(2), 104–110 (2016).
55. S. Lee and C. Park, "Agglomeration of Silica Nanoparticles in Filled Nematic Liquid Crystals," Mol. Cryst. Liq. Cryst. **333**(1), 123–134 (1999).
56. H. Duran, B. Gazdecki, A. Yamashita, and T. Kyu, "Effect of carbon nanotubes on phase transitions of nematic liquid crystals," Liq. Cryst. **32**(7), 815–821 (2005).
57. F. Li, O. Buchnev, C. I. Cheon, A. Glushchenko, V. Reshetnyak, Y. Reznikov, T. J. Sluckin, and J. L. West, "Orientational Coupling Amplification in Ferroelectric Nematic Colloids," Phys. Rev. Lett. **97**(14), 147801 (2006).
58. A. Siarkowska, M. Chychłowski, D. Budaszewski, B. Jankiewicz, B. Bartosewicz, and T. R. Woliński, "Thermo- and electro-optical properties of photonic liquid crystal fibers doped with gold nanoparticles," Beilstein J. Nanotechnol. **8**, 2790–2801 (2017).
59. D. Budaszewski, K. Wolińska, B. Jankiewicz, B. Bartosewicz, and T. R. Woliński, "Spectral Properties of Photo-Aligned Photonic Crystal Fibers Infiltrated with Gold Nanoparticle-Doped Ferroelectric Liquid Crystals," Crystals **10**(9), 785 (2020).